

A Unified Framework for Multimodal, Multi-Part Human Motion Synthesis

Zixiang Zhou
zhouzixiang@xiaobing.ai

Yu Wan
wanyu@xiaobing.ai

Baoyuan Wang
wangbaoyuan@xiaobing.ai



Figure 1. Our unified motion synthesis framework supports multimodal and multi-part human motion generation. Left: text-to-motion. Middle: music-to-motion. Right: speech-to-motion.

Abstract

The field has made significant progress in synthesizing realistic human motion driven by various modalities. Yet, the need for different methods to animate various body parts according to different control signals limits the scalability of these techniques in practical scenarios. In this paper, we introduce a cohesive and scalable approach that consolidates multimodal (text, music, speech) and multi-part (hand, torso) human motion generation. Our methodology unfolds in several steps: We begin by quantizing the motions of diverse body parts into separate codebooks tailored to their respective domains. Next, we harness the robust capabilities of pre-trained models to transcode multimodal signals into a shared latent space. We then translate these signals into discrete motion tokens by iteratively predicting subsequent tokens to form a complete sequence. Finally, we reconstruct the continuous actual motion from this tokenized sequence. Our method frames the multimodal motion generation challenge as a token prediction task, drawing from specialized codebooks based on the modality of the control signal. This approach is inherently scalable, allowing for the easy integration of new modalities. Extensive experiments demonstrated the effectiveness of our design, emphasizing its potential for broad application. Website: <https://zixiangzhou916.github.io/UDE-2/>

1. Introduction

Synthesizing realistic human motion is a pivotal component in many applications, e.g., gaming, virtual reality, and has attracted rising attention in both academia and industry. Recent progress in AI-Generated Content (AIGC) [2, 12, 22, 23, 31, 32, 37, 38] paves a way to generate realistic human motion from various modalities of control signals. These approaches span across handling textual descriptions [22, 23, 31, 37], music clips [30, 32], and speech segments [8, 38]. Despite the advancements, their primary limitation is the focus on single-modality control signals, overlooking the potential of multi-modal integration.

Among various approaches, UDE[37] can synthesize human motion from text or music using one shared model. While its performance is promising, there are several notable limitations: Firstly, it lacks support for speech as a control signal. Secondly, it focuses solely on the torso, neglecting limb articulation such as hand movements. Thirdly, it consolidates the motions of different domains into one universal codebook — a design strategy we later argue is suboptimal. Finally, updating the motion dataset for one domain adversely impacts the other, compromising efficiency and scalability for further enhancements.

The limitations of current methods become pronounced in practical settings such as gaming or filmmaking, where motions may need to be generated from textual cues, mu-

sical scores, or speech. A unified model that can handle these diverse inputs to animate motion would greatly enhance efficiency and practicality. It is equally critical for such a model to prioritize specific body movements depending on the situation; for instance, torso dynamics are crucial in dance sequences, while hand gestures are more prominent during speech. Consequently, a unified approach that can tailor motion synthesis to various body parts, guided by multimodal inputs, is highly valuable.

In this paper, we propose a unified multimodal-driven whole-body motion generation framework to overcome the above limitations. 1) We first learn body part-specific and domain-specific VQ-VAEs to quantize motions of different body parts and different domains into corresponding discrete token representations. 2) To interpret the multimodal control signals effectively, we harness the robust representational capabilities of various large-scale pre-trained models, employing them as encoders for the respective signals. These models generate embedding vectors as latent representations, which are then projected to a uniform dimensionality for seamless integration. 3) To learn the mapping from multimodal embedding representations to multi-part body motions, a multimodal fusion transformer is first adopted. It transforms these embeddings into a joint latent space. Subsequently, we frame the motion synthesis as a language generation task, utilizing discrete codebooks for various body parts and domains as different “vocabulary” in the GPT-like language model[26]. Then we predict the next token from the corresponding “vocabulary” given conditions and past predictions. 4) We decode the predicted token sequences using corresponding decoders to get the final multi-part body motions. To summarize, our significant contributions are outlined as follows:

1. We present a pioneering unified human motion generation model that accepts three distinct modalities: text, music, and speech, and enables the synthesis of diverse body part motions, i.e., the torso and left/right hands.
2. We design novel technical components within our model, including a two-stage VQ-VAE tailored for torso motion quantization and a semantic enhancement loss, both of which significantly elevate the effectiveness.
3. We introduce a weight re-initialization for VQ-VAE training and a semantic-aware sampling technique for diverse generations, to get a further performance boost.
4. Comprehensive evaluations of our method across various tasks – text-driven, music-driven, and speech-driven motion generation – demonstrate its competitive performance and robustness in these domains.

These contributions collectively represent a substantial leap forward in the realm of multimodal human motion generation, showcasing the potential for more nuanced and versatile applications.

2. Related Work

Motion Generation with Text Recent advances in text-based motion generation have streamlined the process from textual descriptions to motion sequences [6, 9, 15, 23, 24, 31, 34, 35, 37]. The major approaches normally employ VAE-based frameworks to encode text into a latent space from which motions are then reconstructed. Concurrently, diffusion models [6, 31] have been adopted, with conditional variants denoising inputs into motion sequences informed by text. Additionally, the influence of language models is evident, with research by [9, 15, 34, 37] and contemporaries quantizing motions into discrete tokens and utilizing autoregressive techniques for generation, predicting each subsequent motion token based on text and prior tokens. Moreover, retrieval-based approaches have also been explored [24, 35]. Here, a database of motions is queried using text-encoded embeddings to find closely aligned motion sequences in the joint latent space, effectively marrying text inputs with pre-existing motion data.

Motion Generation with Music The synthesis of dance movements from music has gained significant interest, employing a variety of techniques. Motion graph methods, as in [3] and [5] segment dances and build graphs for transition between movements based on dynamic and musical styles. These approaches yield high-fidelity dances but necessitate pre-constructed motion graphs. Alternatively, direct generation techniques like those developed by [14],[13], and [32] map music to motion sequences using different architectures: transformer encoder-only, encoder-decoder, and diffusion models, respectively, all focusing on continuous motion prediction from musical inputs. On the other hand, discrete representation is the choice for [30] and [37], where dance moves are not directly derived from music. Instead, these models predict discrete token sequences conditioned on the music, based on which regenerates the dance motion.

Motion Generation with Speech In contrast to text- and music-driven synthesis, speech-driven motion synthesis focuses more on gestural rather than torso movements, with considerable research dedicated to addressing this challenge [1, 2, 4, 8, 20, 25, 33, 38]. Among these methods, diffusion models [1, 4, 33, 38] stand out for their high diversity in generation, as seen in recent works. Yet, these models often lack the capacity for precise editing or specified generation, such as direct manipulation of latent embeddings. On the other hand, variational generative approaches offer an alternative, as explored by [2, 8, 20, 25], where gesture attributes are modulated by distinct latent embeddings produced by dedicated encoders. These models generate gesture movements by integrating all control variables into a continuous representation.

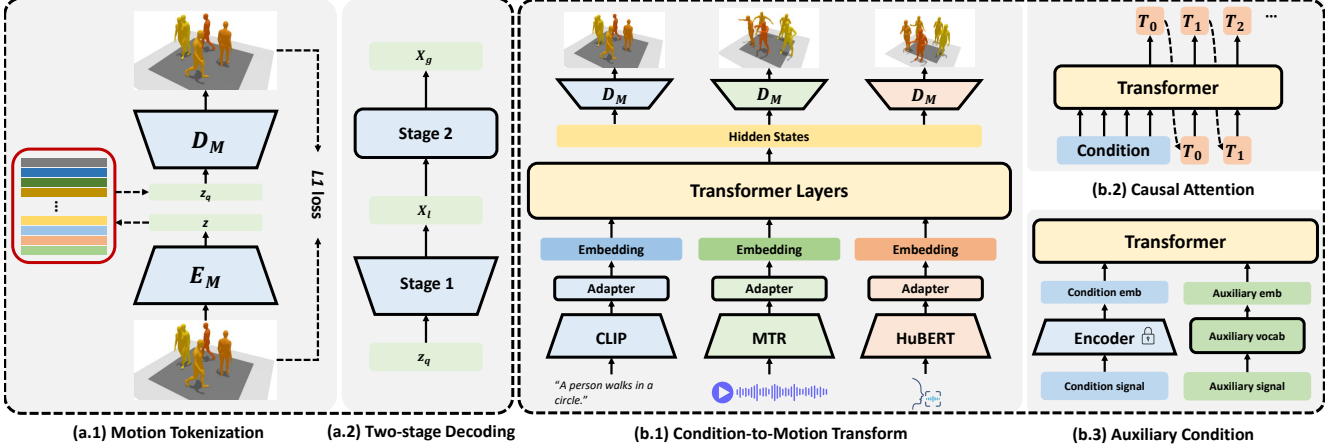


Figure 2. **Overview. a: Hierarchical Motion Tokenization**, where a two-stage motion decoder is introduced to improve the reconstruction quality of torso movements, compared with conventional VQ-VAE. **b: Multimodal Multi-party Motion Synthesis**, including a T5[28]-like architecture for condition-to-motion transform**(b.1)**, a causal attention mechanism**(b.2)** and the fusion of an auxiliary condition **(b.3)**.

The Comparison with Our Work As can be summarized, current human motion generation techniques tend to specialize in single-modality control signals and fail to address multi-part movements. To generate multi-part body movements conditioned on multimodal control signals, different prior methods have to be engineered, making the framework sophisticated and scalable. In contrast, we introduce a unified framework capable of synthesizing diverse body part motions under the guidance of multimodal inputs.

3. Method

The proposed method in Fig. 2 contains two major modules, 1) a hierarchical motion tokenization module that quantizes whole-body motions to separate codebooks, and 2) a multimodal motion generation module that synthesizes whole-body motion tokens based on multimodal conditions.

3.1. Hierarchical Motion Tokenization

We decompose the whole-body pose representation into torso pose and left/right-hand pose representation. Different encoding and decoding strategies are adopted for different body parts.

Hand Motion Tokenization Following the design of VQ-VAE in [37], we learn an encoder $\mathcal{E}(\cdot)$ that transforms hand motion sequence $x \in \mathbb{R}^{T \times c}$ to latent representations $z \in \mathbb{R}^{T' \times d}$, and quantize them by replacing the nearest representation $z^q \in \mathbb{R}^{K \times d}$, where z^q belongs to learned discrete codebook $\mathcal{Z} = \{z_k^q | z_k^q \in \mathbb{R}^{K \times d}\}$.

Hierarchical Torso Motion Tokenization We propose a hierarchical VQ-VAE for torso pose quantization. We use SMPL[18] rotation vector representation for torso poses, each of which is denoted as $x_i = [t_i, r_i]$, where t_i is the root

trajectory, and r_i is the rotation vectors. Instead of feeding $x_i = [t_i, r_i]$ to encoder directly, we use a modified representation: $\bar{x}_i = [\bar{t}_i, r_i]$, where \bar{t}_i is calculated as Eq. 1:

$$\bar{t}_i = \begin{cases} [0, 0, 0], & i = 0, \\ t_i - t_{i-1}, & i > 0. \end{cases} \quad (1)$$

This modification focuses on pose and local trajectory, making the learned discrete representation more robust to global trajectory shifting. We express the encoding as: $z^q = \mathcal{E}(\bar{x})$, where $z \in \mathbb{R}^{T' \times d}$ is the encoded latent representation. We follow the quantization process in [37] to obtain the quantized representation $z^q \in \mathbb{R}^{K \times d}$.

During decoding, we first reconstruct local poses $\bar{y} \in \mathbb{R}^{T \times c}$ as: $\bar{y} = \mathcal{D}_l(z^q)$. For each pose \bar{y}_i , it is expressed as: $\bar{y}_i = [\bar{t}_i, r_i]$. Since we can estimate t_i from \bar{t}_i according to Eq.1, we can, hence, obtain sub-optimal global pose as $\tilde{y} = \mathcal{R}(\bar{y})$, where $\mathcal{R}(\cdot)$ is the reverse process of Eq.1. We refine \tilde{y} using a 1D U-net network to obtain the final pose: $y = \mathcal{D}_g(\tilde{y})$. The two-stage decoding could be expressed as: $y = \mathcal{D}_g(\mathcal{R}(\mathcal{D}_l(z^q)))$. The loss of two-stage VQ-VAE is calculated as Eq. 2:

$$\mathcal{L}_{VQ} = \mathcal{L}_{rec} + \beta_1 \|sg[z] - z_q\| + \beta_2 \|z - sg[z^q]\| \quad (2)$$

where $\mathcal{L}_{rec} = \alpha_1 \mathcal{L}_{rec}^l + \alpha_2 \mathcal{L}_{rec}^{\bar{g}} + \alpha_3 \mathcal{L}_{rec}^g$ is the reconstruction term that contains three sub-items, 1) $\mathcal{L}_{rec}^l = \|\bar{x} - \bar{y}\|$ minimizes the distance between local poses and reconstructed local poses, 2) $\mathcal{L}_{rec}^{\bar{g}} = \|x - \bar{y}\|$ minimizes the distance between global poses and reconstructed sub-optimal global poses, and 3) $\mathcal{L}_{rec}^g = \|x - y\|$ minimizes the global poses and reconstructed global poses. The definition of other two terms $\|sg[z] - z_q\|, \|z - sg[z^q]\|$ follow [37].

Embedding Weights Re-initialization We define the terminology “activated” as if the weight of token embedding is updated during optimization, and it could be decoded back to a valid motion segment. It is non-trivial to tune the factor β_1, β_2 in Eq. 2 to increase the activation rate. We propose a novel training technique, called “weight re-initialization” to solve this problem. For every k step during training, we count the activation rate of every token in the codebook and sort them in descending order, the sorted tokens embeddings are: $[e_i^1, e_j^2, \dots, e_k^n]$, where subscripts i, j, k indicate their original order, and superscripts indicate their sorted order. And the activation rate after sorting follows: $r(e^1) > r(e^2) > \dots > r(e^n)$. We re-initialize the weight of e^k as $e_k \leftarrow e^{n-k} + \delta$ if $r(e^k) < \tau$, where $\delta \sim \mathcal{N}(0, \sigma I)$, and σ is a constant with very small value.

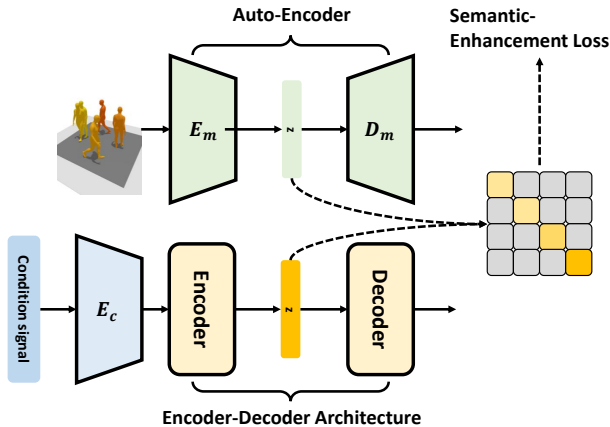


Figure 3. **Pipeline of semantic enhancement.** We propose a novel method to enhance the degree of semantic distinction of condition embedding. We pre-train a motion auto-encoder as prior and use it to enhance the degree of semantic distinction of the hidden states of the encoder part.

3.2. Multimodal Multi-Part Motion Generation

As illustrated in Fig. 2 (b.1), our method supports generating whole-body(torso, left/right hand) motion with three different input modalities. We describe the details below.

Multimodal Alignment We leverage the power of large-scale pre-trained models as modality encoders. We use CLIP text encoder[27] to understand and encode language descriptions. We adopt MTR[7] to encode the music pieces, it is a multimodal model pre-trained on text-music pair data with contrastive loss. We employ HuBERT[11], a self-supervised trained model to learn speech embeddings. For all encoders, we adopt the hidden states of their last layers as the latent embedding sequence. We denote, for modality p , the input condition is $x_p \in \mathbb{R}^{T_p \times c_p}$, the latent embedding is $e_p \in \mathbb{R}^{T'_p \times c'_p}$. We introduce adapter layers to align multimodal embeddings as: $\mathcal{A}_p(e_p) : \mathbb{R}^{T'_p \times c'_p} \rightarrow \mathbb{R}^{T_p \times d}$.

The multimodal alignment could be expressed as: $e_p = \mathcal{A}_p(\mathcal{E}_m(x_p))$.

Hierarchical Condition to Motion Tokens Transform

We adopt an encoder-decoder transformer architecture to transform multimodal conditions to motion tokens. The encoder part takes as input the aligned embeddings $e_p \in \mathbb{R}^{T'_p \times d}$. We pad special tokens to unify the lengths. We extract context information with full attention mechanism and transform it to latent embedding $\tilde{e}_p \in \mathbb{R}^{T'_p \times d}$. Then we employ a transformer decoder to map \tilde{e}_p to motion tokens. We apply causal masks to prevent future information from being leaked in training. We predict the next token successively when generating. We propose a hierarchical decoder architecture to generate tokens of different body parts. Assuming that torso movements depend on the condition and past torso movements, the transform of torso motion tokens is $p_{\theta_t}(x_t) = \prod_{i=1}^n p_{\theta_t}(x_{t,i} | x_{t,<i}, C)$, where C is condition. Same assumption holds for hands movements as: $p_{\theta_h}(x_h) = \prod_{i=1}^n p_{\theta_h}(x_{h,i} | X_{h,<i}, C)$. In our hierarchical design, we adopt a base decoder to learn the common latent information. We use separate head decoders to learn part-specific and modality-specific motion tokens. Therefore, the hierarchical condition-to-motion transform could be written as:

$$p(x_{b,p}) = \prod_{i=1}^n p_{\theta}(x_{b,p,i} | X_{b,p,<i}, C_p) p_{\theta_{b,p}}(x_{b,p,i} | X_{b,p,<i}, C_p) \quad (3)$$

In Eq. 3, b denotes body parts, and p denotes modality of the condition, θ denotes the parameters of base decoder, and $\theta_{b,p}$ denotes the parameters of head decoders.

Separate Motion Vocabulary

We use separate vocabulary for different body parts subject to different modalities. The use of separate vocabulary brings several advantages, 1) it avoids sampling out-of-domain motion tokens, 2) updating the vocabulary of one domain will not affect the others, and 3) it is efficient to introduce additional modality to our pipeline as a plug-in.

Alignment of Auxiliary Condition

Our method supports taking any auxiliary conditions as a supplement. For instance, when generating gesture motion from speech, the persona of characters matters. We introduce trainable auxiliary vocabulary to the encoder part as $\mathcal{Z}_{aux} = \{e_{aux} | e_{aux} \in \mathbb{R}^{K \times d}\}$, where K is the number of auxiliary conditions, and d is the latent dimension. We append the auxiliary embedding e_{aux} to dominant condition embeddings e_m as: $e_{fused} = [e_m, e_{aux}]$, shown in Fig. 2 (b.3).

Semantic Enhancement

Semantic meaning of condition signal plays a vital role in generating human motion. It is self-explanatory that conditions with opposite semantic meanings should correspond to human movements of obvious difference. For instance, the human motions described

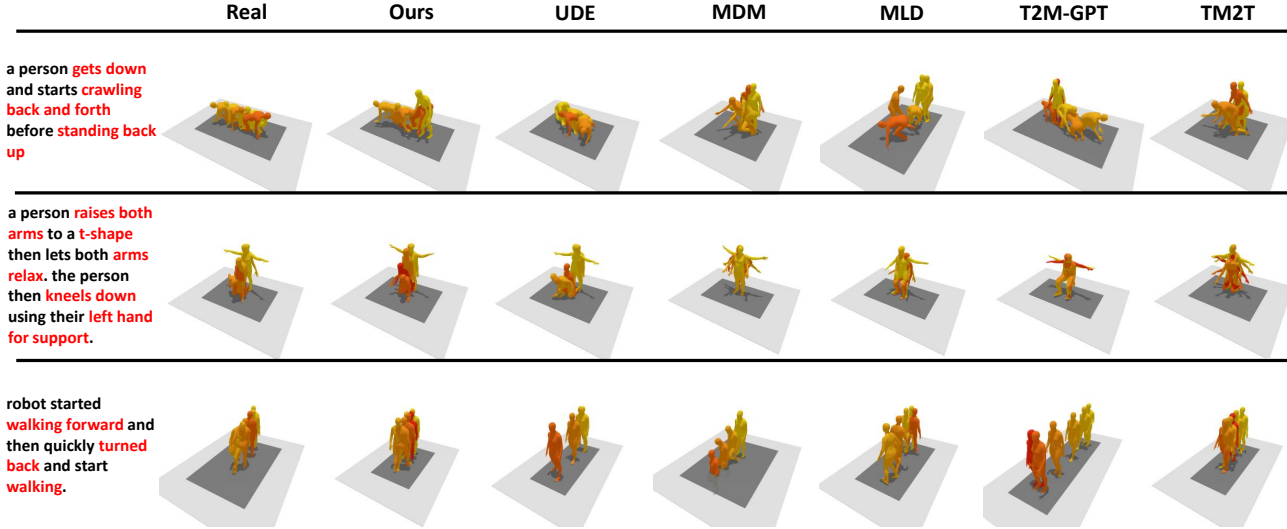


Figure 4. **Visual Comparison on Text-to-Motion Task.** We evenly show 5 poses for each motion to compare ours with SOTAs on text-to-motion tasks. The condition language descriptions are shown in the very left column. Keywords are highlighted.

Method	R Precision					FID ↓	Div →	MM ↑
	Top-1 ↑	Top-2 ↑	Top-3 ↑	Top-4 ↑	Top-5 ↑			
GT	63.49	78.50	84.66	88.14	90.35	0.082	14.45	-
TM2T[9]	42.27±1.137	57.04±1.200	65.10±1.293	70.58±1.285	74.82±1.313	10.80±0.065	13.77±0.058	1.62±0.342
MDM[31]	48.88±1.121	65.53±1.200	72.81±1.293	78.12±1.335	81.47±1.281	4.53±0.034	13.88±0.034	7.12±0.071
T2M-GPT[34]	51.36±1.187	64.85±1.217	75.88±1.140	78.75±1.136	82.32±1.177	6.67±0.061	13.65±0.219	5.65±0.229
MLD[6]	48.85±0.996	65.52±1.096	73.21±1.326	78.52±1.143	80.97±1.246	11.85±0.097	13.64±0.219	4.63±1.655
UDE[37]	46.69±1.152	61.69±1.259	69.82±1.239	75.04±1.240	78.61±1.236	2.57±0.019	14.25±0.034	6.83±0.121
Ours	54.48±0.340	68.02±0.280	74.50±0.280	78.62±0.240	81.63±0.230	2.54±0.045	14.72±0.034	8.48±0.297

Table 1. **Results of text-to-motion.** We compare the results of text-to-motion generation between ours and the SOTA methods. Our method achieves better semantic relevance, fidelity, and diversity performances. Indicate best results , indicates second best results .

by C_1 : “a person is running forward” and C_2 : “a person is running backward” should present remarkable difference, while the motion described by C_3 : “a person is walking forward” is expected to be more similar with the one described by C_1 than C_2 . We denote the motion generated by condition C as x_c , the similarity between two motion sequences and conditions are $s_m = \langle x_{c_1}, x_{c_2} \rangle$ and $s_c = \langle c_1, c_2 \rangle$. We empirically found that for any two pairs of $\{x_c, c\}$, $s_m \propto s_c$ does not hold. It is particularly obvious for text-to-motion scenarios. We propose a novel semantic enhancement loss to facilitate the alignment between motion and condition. As shown in Fig. 3, we pre-train a motion auto-encoder and use its encoder to encode motion as $e_m \in \mathbb{R}^{1 \times d}$. We denote $e_c \in \mathbb{R}^{1 \times d}$ as temporal average of condition embeddings $\tilde{e}_p \in \mathbb{R}^{T_p \times d}$ obtained by condition-to-motion encoder transformer. We align e_m and e_c in latent space by maximizing the cross-modality similarity. Specifically, we fix the motion encoder and optimize the condition-to-motion encoder to align e_c to e_m . This benefits learning motion-aware representation from the condition. Our semantic enhancement loss is:

$$\mathcal{L}_{sem} = \frac{1}{N} \sum_{i=1}^N (1 - \langle s_m^i, s_c^i \rangle) \quad (4)$$

Semantic-Aware Sampling We propose a simple yet efficient sampling approach called “semantic-aware sampling” to boost the semantic correlation while maintaining generation diversity. We found that the token embedding similarity is proportional to motion dynamic similarity. Instead of sampling a token from a probability distribution, we sample one token using a different approach. Suppose token y_i corresponds to the largest probability $p(x_i | x_1, x_2, \dots, x_{i-1}, C)$, and its embedding in codebook is z_i^q . We calculate the pairwise distance between z_i^q and $\{z_j^q\}_{j=1}^K$ as: $d_{ij}(z_i^q, z_j^q) = \|z_i^q - z_j^q\|_2$. Then convert the distance to weight factors as:

$$w_{ij} = \frac{\exp(-d_{ij}/t)}{\sum_{j=1}^K \exp(-d_{ij}/t)} \quad (5)$$

where t is the temperature coefficient. Multiplying weight w by probability p adjusts the distribution by reducing the probability that dynamically irrelevant tokens have been sampled. Hence, increasing the semantic consistency.

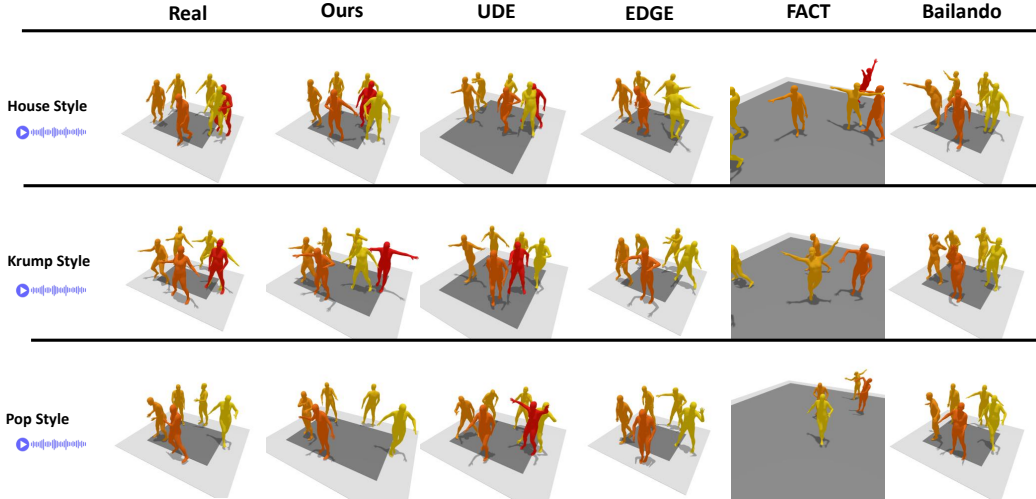


Figure 5. **Visual Comparison on Music-to-Motion Task.** To ease the visualization, we modify the trajectory of each dance movement and present 5 poses per sequence.

Method	MDSC				FID ↓	Div →	MM ↑	BAS ↑
	Acc. ↑	Top-1 Retr. ↑	I2I. ↓	Simi. ↑				
GT	38.32	37.65	0.72	0.48	1.03	2.19	-	0.237
FACT[14]	17.67	17.96	0.92	0.01	2.43	2.89	-	0.221
Bailando[30]	37.04	38.01	0.74	0.32	1.04	2.12	-	0.233
UDE[37]	20.69±4.231	19.84±3.902	0.89	0.17	0.38±0.015	2.04±0.014	1.85 ^{0.007}	0.231±0.019
EDGE[32]	23.93±2.404	23.69±2.211	0.86	0.41	1.17±0.015	1.85±0.016	1.68±0.092	0.260
Ours	54.25±4.564	53.89±4.119	0.56	0.60	0.46±0.023	2.06±0.021	1.75±0.028	0.222±0.025

Table 2. **Results of music-to-motion.** We compare the style consistency, motion quality, and diversity between ours and previous methods and the results suggest that our method achieves the highest consistency. Indicate best results , indicates second best results .

Method	ID Consis.		FID ↓	Div →	MM ↑
	Acc. ↑	I2I. ↓			
GT	99.97	0.36	0.36	2.26	-
DSG[33]	99.91±0.000	0.44±0.000	0.55±0.000	2.18±0.000	1.80±0.005
Ours	93.16±7.900	0.46±0.051	0.75±0.054	2.37±0.018	2.01±0.006

Table 3. **Results of speech-to-motion.** We evaluate the ID consistency, motion quality, and diversity between our and SOTA methods. Indicate best results , indicates second best results .

4. Experiments

4.1. Datasets and Preprocessing

We utilize HumanML3D[10] and AIST++[14] for text-conditioned and music-conditioned task respectively. For speech-conditioned tasks, we use BEAT[17], a large-scale conversational gesture synthesis dataset. We follow [37] to preprocess the HumanML3D and AIST++ datasets, resulting in motion sequences with identical representation. For BEAT[17], we use the same motion representation for the body sequences, and for left hand and right hand, we use MANO[29] representation with 12 PCA components for each hand. Because BEAT has a large amount of data,

we only use data corresponding to 4 IDs for training and evaluation (ID: 2, 4, 6, 8). For music and speech data, we use raw acoustic wave sampled as 16KHz.

4.2. Implementation Details

For tokenization, the codebook size of body parts is set to 1024 for all text-, music-, and speech-conditioned generations. The codebook size of hand parts is 512. The embedding dimensions are 512 for all. We train 500 epochs for VQ-VAEs. For condition-to-motion transform, the encoder part is an 8-layer transformer encoder, the base decoder part is a 6-layer transformer decoder, and the head decoder parts are a 2-layer transformer decoder, respectively. We don't train our model on multi-domain data jointly at first. We train it on HumanML3D[10] for 200 epochs, then we integrate AIST++[14] to continue training for 1000 epochs, then we add BEAT[17] for another 1000 epochs.

4.3. Evaluation Metrics

Text-to-Motion We use Frechet Inception Distance (FID) to measure the distance between generated motion and the real motion distributions, and diversity (Div) to measure the feature distance among all generated motion sequences. We

Method		HumanML3D[9]				AIST++[14]				BEAT[17]			
Two-stage	Re-init.	FID ↓	MPJPE ↓	MPJVE ↓	MPJAE ↓	FID ↓	MPJPE ↓	MPJVE ↓	MPJAE ↓	FID ↓	MPJPE ↓	MPJVE ↓	MPJAE ↓
✓	✗	1.807	0.100	0.012	0.012	5.449	0.154	0.017	0.013	0.682	0.018	0.0018	0.0013
✗	✓	1.693	0.072	0.010	0.008	5.278	0.090	0.014	0.010	0.726	0.019	0.0018	0.0012
✓	✓	1.167	0.054	0.007	0.004	5.193	0.087	0.012	0.007	0.518	0.018	0.0017	0.0011

Table 4. **Ablation Study on Variants VQ-VAE Designs.** The results suggest two-stage design and re-initialization strategy improve the performance well. Indicate best results .

Method	Text-to-Motion				Music-to-Motion				Speech-to-Motion			
	Top-1 ↑	Top-3 ↑	FID ↓	MM ↑	Acc. ↑	I2I. ↓	FID ↓	MM ↑	Acc. ↑	I2I. ↓	FID ↓	MM ↑
w/o SemE.	53.99	74.22	2.57	-	54.14	0.56	0.44	-	94.48	0.50	0.66	-
w/ SemE.	55.06	75.60	2.56	-	54.29	0.55	0.60	-	93.92	0.49	0.83	-
w/o SaS.	52.71	73.06	2.48	9.02	53.85	0.57	0.53	1.86	92.61	0.49	0.89	2.02
w/ SaS.	54.48	74.50	2.54	8.48	54.25	0.56	0.46	1.75	93.16	0.47	0.75	2.01

Table 5. **Ablation Study on Semantic Enhancement and Semantic-aware Sampling.** We found semantic enhancement improves the semantic correlation and fidelity for the text-to-motion domain. And semantic-aware sampling brings semantic correlation gain with less fidelity and diversity loss on three domains. Indicate best results .

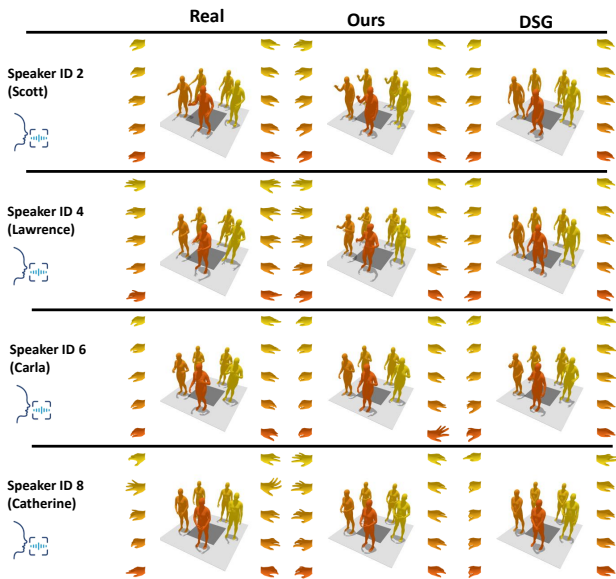


Figure 6. **Visual Comparison on Speech-to-Motion Task.** To ease the visualization, we modify the trajectory of each dance movement and present 5 poses per sequence. We enlarge the display of hand motions and show them on both sides of the whole-body motion display.

use multimodality (MM) to measure the diversity of motions conditioned on the same textual description. Finally, we measure the motion-text semantic correlation using **R-Precision**[10]. Inspired by [24][19], we train a text-motion alignment model for evaluating R-Precision. The detail of this model is described in Appendix.

Music-to-Motion We use **FID**, **Div** and **MM** for motion quality, diversity measurement. We use beat alignment score(**BAS**)[14] to measure the alignment between motion

and music beat. In addition, we use **MDSC**[36] to measure the stylistic alignment between generated dance movements and music pieces.

Speech-to-Motion Similarly, we use **FID** for quality measurement, **Div** and **MM** for diversity measurement. We observe that personality affects the motion patterns a lot in speech-driven scenarios, it is beneficial if we can measure the ID consistency. Inspired by [36], we proposed a metric to measure the alignment between motion and ID. We describe the detail in Appendix.

4.4. Results

We evaluate our method on three tasks, 1) text-to-motion, 2) music-to-motion, 3) speech-to-motion, and compare our method with several SOTAs[6, 9, 23, 31, 34, 37] respectively. We discuss them in detail as follows.

Comparison on Text-to-Motion For the text-to-motion task, We reproduce the SOTAs following their official implementations using rotation vector as motion representation. We argue that this setting eliminates the effect of different motion representations. The comparison results are reported in Tab. 1, which suggests our method has a better capability of mapping the semantic meaning of condition language descriptions to motion sequences. Meanwhile, our method achieves better motion quality and diversity compared with SOTAs. Fig. 4 shows a few examples for visual comparison.

Comparison on Music-to-Motion We reproduce [14, 30, 32, 37] to compare with ours. For every piece of condition music, we generate dance sequences with the same length as input music using our method and SOTAs. We crop the motion sequences to consecutive 5sec segments and evaluate the metrics on these segments. Tab. 2 shows

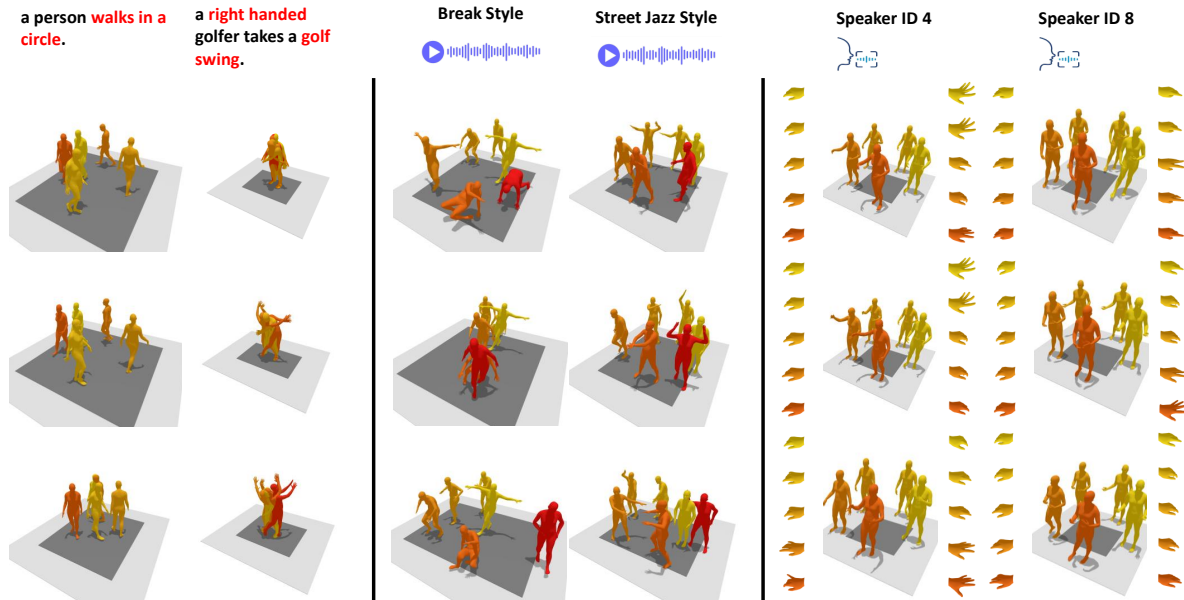


Figure 7. **Diverse Generated Motions.** We generate 3 motion sequences from the same condition to present that our method has promising ability of diverse generation. **Left:** text-to-motion. **Middle:** music-to-motion. **Right:** speech-to-motion.

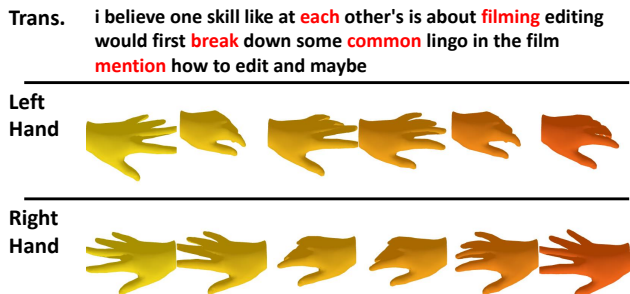


Figure 8. **Hands Motion Generation.** We evenly visualize 6 poses from a 10-second motion. The transcription is also shown at the top row and keywords corresponding to selected frames are highlighted.

that our method has stronger ability in generating style-consistent dance movements from music pieces than others while achieving competitive results in fidelity and diversity. Fig. 5 also provides visual comparison results to facilitate assessment.

Comparison on Speech-to-Motion We compare ours with [33] on BEAT[17] using SMPL-X[21] representation. It contains torso and left/right-hand motions. We generate long whole-body motion sequences and crop to multiple 5sec segments for evaluation. We show the results in Tab. 3 and the visual comparison in Fig. 6. Specifically, we show in Fig. 8 that our method can synthesize vivid and smooth hand motions from speech signals.

4.5. Ablation Study

For ablations, we validated the effectiveness of the two-stage VQ-VAE and the weight re-initialization technique. Tab. 4 shows that applying both techniques boosts the reconstruction quality of VQ-VAE on all three datasets.

We also investigate the effectiveness of two modules proposed in condition-to-motion transform, 1) semantic enhancement (SemE.), and 2) semantic-aware sampling (SaS.). The ablation results are presented in Tab. 5. We found that SemS. consistently improves the semantic correlation and fidelity for the text-to-motion domain, while this tendency is not obvious for music-conditioned and speech-conditioned domains. We will discuss this in detail in the Appendix. The SaS. brings semantic correlation gain with limited fidelity and diversity loss on three domains.

5. Conclusion

In this paper, we propose a unified framework that supports synthesizing whole-body human motions with up to 3 modalities of control signals. We adopt separate codebooks and use a two-stage VQ-VAE and re-initialization strategy to improve the motion quantization quality. In addition, we utilize an encoder-decoder architecture to transform multi-modal conditions into motion tokens. Meanwhile, we propose a semantic enhancement module to advance the semantic relevance and also introduce a semantic-aware sampling technique to further boost the correlation with limited fidelity and diversity loss. Extensive evaluation suggests our method achieves state-of-the-art in all domains.

References

- [1] Simon Alexanderson, Rajmund Nagy, Jonas Beskow, and Gustav Eje Henter. Listen, denoise, action! audio-driven motion synthesis with diffusion models. *ACM Transactions on Graphics (TOG)*, 42(4):1–20, 2023. [2](#)
- [2] Tenglong Ao, Qingzhe Gao, Yuke Lou, Baoquan Chen, and Libin Liu. Rhythmic gesticulator: Rhythm-aware co-speech gesture synthesis with hierarchical neural embeddings. *ACM Transactions on Graphics (TOG)*, 41(6):1–19, 2022. [1](#), [2](#)
- [3] Ho Yin Au, Jie Chen, Junkun Jiang, and Yike Guo. Choreograph: Music-conditioned automatic dance choreography over a style and tempo consistent dynamic graph. In *Proceedings of the 30th ACM International Conference on Multimedia*, pages 3917–3925, 2022. [2](#)
- [4] Ankur Chemburkar, Shuhong Lu, and Andrew Feng. Discrete diffusion for co-speech gesture synthesis. In *GENEA: Generation and Evaluation of Non-verbal Behaviour for Embodied Agents Challenge 2023*, 2023. [2](#)
- [5] Kang Chen, Zhipeng Tan, Jin Lei, Song-Hai Zhang, Yuan-Chen Guo, Weidong Zhang, and Shi-Min Hu. Choreomaster: choreography-oriented music-driven dance synthesis. *ACM Transactions on Graphics (TOG)*, 40(4):1–13, 2021. [2](#)
- [6] Xin Chen, Biao Jiang, Wen Liu, Zilong Huang, Bin Fu, Tao Chen, and Gang Yu. Executing your commands via motion diffusion in latent space. In *Proceedings of the IEEE/CVF Conference on Computer Vision and Pattern Recognition*, pages 18000–18010, 2023. [2](#), [5](#), [7](#)
- [7] SeungHeon Doh, Minz Won, Keunwoo Choi, and Juhan Nam. Toward universal text-to-music retrieval. In *ICASSP 2023-2023 IEEE International Conference on Acoustics, Speech and Signal Processing (ICASSP)*, 2023. [4](#)
- [8] Saeed Ghorbani, Ylva Ferstl, Daniel Holden, Nikolaus F Troje, and Marc-André Carbonneau. Zeroeggs: Zero-shot example-based gesture generation from speech. In *Computer Graphics Forum*, pages 206–216. Wiley Online Library, 2023. [1](#), [2](#)
- [9] Chuan Guo, Xinxin Xuo, Sen Wang, and Li Cheng. Tm2t: Stochastic and tokenized modeling for the reciprocal generation of 3d human motions and texts. *arXiv preprint arXiv:2207.01696*, 2022. [2](#), [5](#), [7](#)
- [10] Chuan Guo, Shihao Zou, Xinxin Zuo, Sen Wang, Wei Ji, Xingyu Li, and Li Cheng. Generating diverse and natural 3d human motions from text. In *Proceedings of the IEEE/CVF Conference on Computer Vision and Pattern Recognition*, pages 5152–5161, 2022. [6](#), [7](#), [13](#)
- [11] Wei-Ning Hsu, Benjamin Bolte, Yao-Hung Hubert Tsai, Kushal Lakhotia, Ruslan Salakhutdinov, and Abdelrahman Mohamed. Hubert: Self-supervised speech representation learning by masked prediction of hidden units. *IEEE/ACM Transactions on Audio, Speech, and Language Processing*, 29:3451–3460, 2021. [4](#), [11](#)
- [12] Ruozi Huang, Huang Hu, Wei Wu, Kei Sawada, Mi Zhang, and Daxin Jiang. Dance revolution: Long-term dance generation with music via curriculum learning. *arXiv preprint arXiv:2006.06119*, 2020. [1](#)
- [13] Buyu Li, Yongchi Zhao, Shi Zhelun, and Lu Sheng. Danceformer: Music conditioned 3d dance generation with parametric motion transformer. In *Proceedings of the AAAI Conference on Artificial Intelligence*, pages 1272–1279, 2022. [2](#)
- [14] Ruilong Li, Shan Yang, David A Ross, and Angjoo Kanazawa. Ai choreographer: Music conditioned 3d dance generation with aist++. In *Proceedings of the IEEE/CVF International Conference on Computer Vision*, pages 13401–13412, 2021. [2](#), [6](#), [7](#), [13](#)
- [15] Junfan Lin, Jianlong Chang, Lingbo Liu, Guanbin Li, Liang Lin, Qi Tian, and Chang-wen Chen. Being comes from not-being: Open-vocabulary text-to-motion generation with wordless training. In *Proceedings of the IEEE/CVF conference on computer vision and pattern recognition*, pages 23222–23231, 2023. [2](#)
- [16] Jing Lin, Ailing Zeng, Shunlin Lu, Yuanhao Cai, Ruimao Zhang, Haoqian Wang, and Lei Zhang. Motion-x: A large-scale 3d expressive whole-body human motion dataset. *Advances in Neural Information Processing Systems*, 2023. [13](#)
- [17] Haiyang Liu, Zihao Zhu, Naoya Iwamoto, Yichen Peng, Zhengqing Li, You Zhou, Elif Bozkurt, and Bo Zheng. Beat: A large-scale semantic and emotional multi-modal dataset for conversational gestures synthesis. In *European Conference on Computer Vision*, pages 612–630. Springer, 2022. [6](#), [7](#), [8](#)
- [18] Matthew Loper, Naureen Mahmood, Javier Romero, Gerard Pons-Moll, and Michael J. Black. SMPL: A skinned multi-person linear model. *ACM Trans. Graphics (Proc. SIGGRAPH Asia)*, 34(6):248:1–248:16, 2015. [3](#)
- [19] Shunlin Lu, Ling-Hao Chen, Ailing Zeng, Jing Lin, Ruimao Zhang, Lei Zhang, and Heung-Yeung Shum. Humantomato: Text-aligned whole-body motion generation. *arXiv preprint arXiv:2310.12978*, 2023. [7](#)
- [20] Kunkun Pang, Dafei Qin, Yingruo Fan, Julian Habekost, Takaaki Shiratori, Junichi Yamagishi, and Taku Komura. Bodyformer: Semantics-guided 3d body gesture synthesis with transformer. *ACM Transactions on Graphics (TOG)*, 42(4):1–12, 2023. [2](#)
- [21] Georgios Pavlakos, Vasileios Choutas, Nima Ghorbani, Timo Bolkart, Ahmed A. A. Osman, Dimitrios Tzionas, and Michael J. Black. Expressive body capture: 3d hands, face, and body from a single image. In *Proceedings IEEE Conf. on Computer Vision and Pattern Recognition (CVPR)*, 2019. [8](#)
- [22] Mathis Petrovich, Michael J Black, and Gül Varol. Action-conditioned 3d human motion synthesis with transformer vae. In *Proceedings of the IEEE/CVF International Conference on Computer Vision*, pages 10985–10995, 2021. [1](#), [11](#)
- [23] Mathis Petrovich, Michael J Black, and Gül Varol. Temos: Generating diverse human motions from textual descriptions. *arXiv preprint arXiv:2204.14109*, 2022. [1](#), [2](#), [7](#)
- [24] Mathis Petrovich, Michael J Black, and Gül Varol. Tmr: Text-to-motion retrieval using contrastive 3d human motion synthesis. *arXiv preprint arXiv:2305.00976*, 2023. [2](#), [7](#)
- [25] Xingqun Qi, Chen Liu, Lincheng Li, Jie Hou, Haoran Xin, and Xin Yu. Emotiongesture: Audio-driven diverse emotional co-speech 3d gesture generation. *arXiv preprint arXiv:2305.18891*, 2023. [2](#)

- [26] Alec Radford, Karthik Narasimhan, Tim Salimans, Ilya Sutskever, et al. Improving language understanding by generative pre-training. 2018. [2](#)
- [27] Alec Radford, Jong Wook Kim, Chris Hallacy, Aditya Ramesh, Gabriel Goh, Sandhini Agarwal, Girish Sastry, Amanda Askell, Pamela Mishkin, Jack Clark, et al. Learning transferable visual models from natural language supervision. In *International Conference on Machine Learning*, pages 8748–8763. PMLR, 2021. [4](#), [11](#)
- [28] Colin Raffel, Noam Shazeer, Adam Roberts, Katherine Lee, Sharan Narang, Michael Matena, Yanqi Zhou, Wei Li, and Peter J. Liu. Exploring the limits of transfer learning with a unified text-to-text transformer. *Journal of Machine Learning Research*, 21(140):1–67, 2020. [3](#)
- [29] Javier Romero, Dimitrios Tzionas, and Michael J. Black. Embodied hands: Modeling and capturing hands and bodies together. *ACM Transactions on Graphics, (Proc. SIGGRAPH Asia)*, 36(6), 2017. [6](#)
- [30] Li Siyao, Weijiang Yu, Tianpei Gu, Chunze Lin, Quan Wang, Chen Qian, Chen Change Loy, and Ziwei Liu. Bailando: 3d dance generation by actor-critic gpt with choreographic memory. In *Proceedings of the IEEE/CVF Conference on Computer Vision and Pattern Recognition*, pages 11050–11059, 2022. [1](#), [2](#), [6](#), [7](#)
- [31] Guy Tevet, Sigal Raab, Brian Gordon, Yonatan Shafir, Daniel Cohen-Or, and Amit H Bermano. Human motion diffusion model. *arXiv preprint arXiv:2209.14916*, 2022. [1](#), [2](#), [5](#), [7](#)
- [32] Jonathan Tseng, Rodrigo Castellon, and Karen Liu. Edge: Editable dance generation from music. In *Proceedings of the IEEE/CVF Conference on Computer Vision and Pattern Recognition*, pages 448–458, 2023. [1](#), [2](#), [6](#), [7](#)
- [33] Sicheng Yang, Zhiyong Wu, Minglei Li, Zhensong Zhang, Lei Hao, Weihong Bao, Ming Cheng, and Long Xiao. Diffusestylegesture: Stylized audio-driven co-speech gesture generation with diffusion models. *arXiv preprint arXiv:2305.04919*, 2023. [2](#), [6](#), [8](#)
- [34] Jianrong Zhang, Yangsong Zhang, Xiaodong Cun, Shaoli Huang, Yong Zhang, Hongwei Zhao, Hongtao Lu, and Xi Shen. T2m-gpt: Generating human motion from textual descriptions with discrete representations. *arXiv preprint arXiv:2301.06052*, 2023. [2](#), [5](#), [7](#)
- [35] Mingyuan Zhang, Xinying Guo, Liang Pan, Zhongang Cai, Fangzhou Hong, Huirong Li, Lei Yang, and Ziwei Liu. Remodiffuse: Retrieval-augmented motion diffusion model. *arXiv preprint arXiv:2304.01116*, 2023. [2](#)
- [36] Zixiang Zhou and Baoyuan Wang. Mdsc: Towards evaluating the style consistency between music and dance. *arXiv preprint arXiv:2309.01340*, 2023. [7](#), [11](#)
- [37] Zixiang Zhou and Baoyuan Wang. Ude: A unified driving engine for human motion generation. In *Proceedings of the IEEE/CVF Conference on Computer Vision and Pattern Recognition*, pages 5632–5641, 2023. [1](#), [2](#), [3](#), [5](#), [6](#), [7](#)
- [38] Lingting Zhu, Xian Liu, Xuanyu Liu, Rui Qian, Ziwei Liu, and Lequan Yu. Taming diffusion models for audio-driven co-speech gesture generation. In *Proceedings of the IEEE/CVF Conference on Computer Vision and Pattern Recognition*, pages 10544–10553, 2023. [1](#), [2](#)

Supplementary Material

A. Text-Motion Alignment Model

Fig. 9 shows our approach in evaluating motion-to-text consistency. We encode the motion sequence and text description to embeddings z_m and z_t , respectively. And measure the cosine similarity as the degree of alignment between motion and text. We first train a motion auto-encoder and use its encoder to encode the motion sequence. We adopt the model design proposed in [22]. For the text encoder, we use the pretrained CLIP[27] text encoder to encode the text description. As discussed previously(Section 3.2), the semantic discrepancy between motion and text exists. We show how to train the text-motion alignment model in Fig. 9 (c). We introduce two adapter layers, they transform the embeddings obtained by motion and text encoder z_m and z_t to the same dimension. To align them in semantically meaningful latent space, we regularize them through reconstructing motion from aligned embeddings. During the training, we initialize the encoders and decoders with their pretrained weights. We fix the CLIP text encoder, and we tune the pretrained motion encoder and decoder with a small learning rate. We train the adapter layers with a relatively large learning rate. The alignment model is trained by optimizing the following objective:

$$\mathcal{L} = \mathcal{L}_{recon} + \mathcal{L}_{infoNCE} \quad (6)$$

Where

$$\mathcal{L}_{recon} = \|x - \tilde{x}\|_2 \quad (7)$$

is the reconstruction term, and

$$\mathcal{L}_{infoNCE} = -\frac{1}{N} \sum_{i=1}^K \left(\log \frac{\exp(\langle z_m^i, z_t^i \rangle / \tau)}{\exp(\sum_{j=1}^K \langle z_m^i, z_t^j \rangle / \tau)} \right) \quad (8)$$

is the infoNCE loss which helps align paired text-motion close while pushing unpaired apart.

We compare different models and training designs as motion-text alignment models in Tab. 6. It is noticeable that tuning pretrained E_m and D_m with a small learning rate brings remarkable performance improvement, which proves the effectiveness of our design.

B. Speech-to-Motion ID Consistency Evaluation Model

We argue that the characters of speakers affect the motion patterns severely in terms of the speech-to-motion domain. We propose a novel method to evaluate ID consistency. Inspired by [36], we formulate it as a clustering problem. Specifically, if motions could be encoded to latent representation embeddings, embeddings corresponding to the motions performed by the same person should be close to each other in latent space, while those corresponding to different

Variants		R Top-1 ↑	R Top-2 ↑	R Top-3 ↑	R Top-4 ↑	R Top-5 ↑
tune E_m	tune D_m					
✗	✗	19.85	29.18	35.25	40.58	45.18
✗	✓	50.96	66.13	73.67	78.72	82.40
✓	✓	63.60	79.23	85.02	88.14	90.44

Table 6. **Comparison on Text-Motion Alignment.** We compare different models and training designs on the text-motion alignment model. We found tuning E_m and D_m brings significant performance gain. Indicate best results .

persons should be away from each other. This is a typical clustering hypothesis. Fig. 10 shows the proposed model. We propose two metrics to assess ID consistency. 1) I2I: measures the ratio between intra-cluster to inter-cluster distance. Given a target motion, its representation is encoded by pretrained motion encoder as z_m . We calculate the intra-cluster distance as: $d_{intra} = \|z_m - \hat{z}_m^i\|_2$, where \hat{z}_m^i is the learned cluster center of ID i , and the inter-cluster distance is calculated as: $d_{inter} = \frac{1}{N-1} \sum_{j=1, j \neq i}^N (\|z_m^i - \hat{z}_m^j\|_2)$. Smaller I2I indicates higher ID consistency. 2) Acc: measure the ID prediction accuracy. We first train a motion auto-encoder, then we fix the encoder and a pretrained speech encoder[11] as encoder priors. We use two adapter layers to align the speech and motion embeddings in latent space. These adapter layers are only trainable modules here, and we train them using clustering loss and cross-entropy loss(Fig. 10 (c)).

C. More Results of Ablation Study

Weights Re-Initialization We compare the activation rate of codebook tokens with and without using the weights re-initialization strategy on three datasets. Fig. 12 presents the comparison results. We encode the test sets and count the activation rate. We sort the results according to the activation rate in descending order and display them in a histogram-like style. It is clearly observed that the weights re-initialization strategy increases the code activation rate remarkably.

Semantic Enhancement We investigate the effectiveness of the proposed semantic enhancement module. It is discussed previously that semantic enhancement is particularly effective in the text-motion domain, while large-scale pre-trained models like CLIP[27] are not able to capture the semantics accurately in some cases. For instance, Fig. 11 (a) shows the semantic similarity between embeddings encoded by CLIP. The associated textual descriptions are shown in Fig. 11 (d). As we can see, CLIP text encoder fails to understand the key semantics. For example, ‘a person walks forward quickly’ and ‘a person walks backward

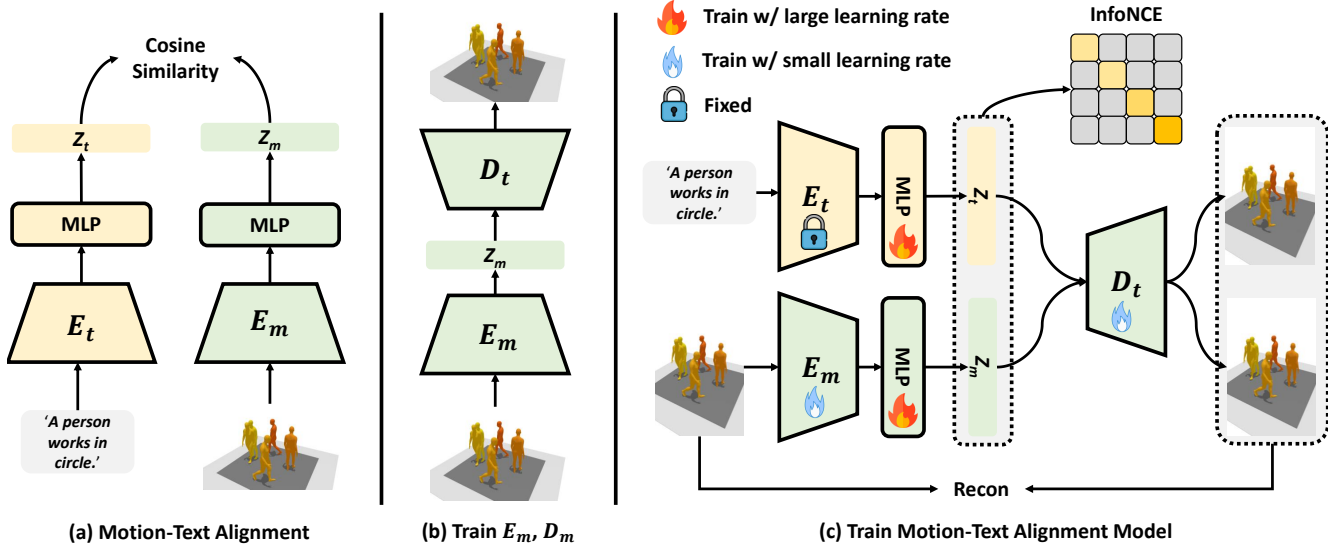


Figure 9. **Pipeline of Text-Motion Alignment Model.** (a) Measuring the cosine similarity as text-motion alignment. (b) Pretrain motion auto-encoder. (c) Train the text-motion alignment model using reconstruction and infoNCE loss.

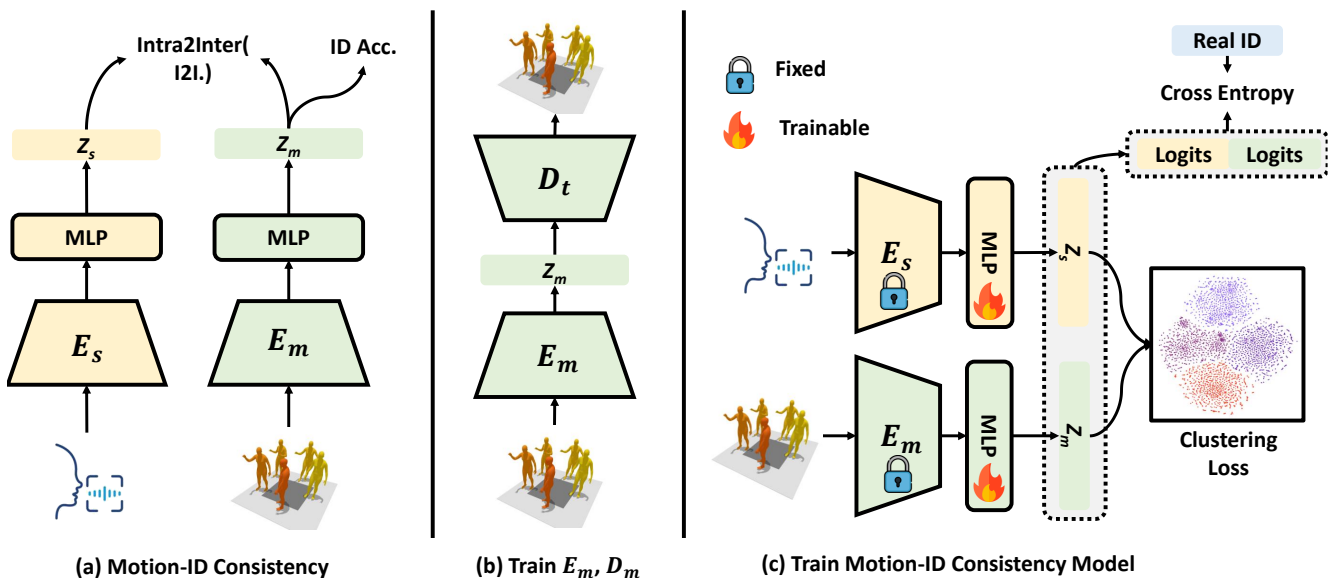


Figure 10. **Pipeline of Speech-to-Motion ID Consistency Model.** (a) Measuring the Intra2Inter(I2I.) and ID prediction accuracy(ID Acc.) as metrics. (b) Pretrain motion auto-encoder. (c) Train the speech-to-motion ID consistency model using clustering loss and cross entropy loss.

quickly’ have very similar expressions, but their semantics vary a lot. But the similarity shows that ‘a person walks forward quickly’ is closer to ‘a person walks backward quickly’ than ‘a person is running forward quickly’. We believe that this is because CLIP is trained on a pair of static images and text, and the dynamic semantics in the text is not well learned as a result. We show in Fig. 11 (b), (c) that our proposed semantic enhancement loss helps to learn better semantics from textual description. For instance, it helps

distinguish the semantics from ‘forward’ and ‘backward’ accurately.

D. More Results on Motion Generation

We present more motion generation results in Fig. 13, 14, 15. For the text-to-motion domain, we show 16 motion sequences synthesized by different textual descriptions. For the music-to-motion domain, we select 8 genres and show

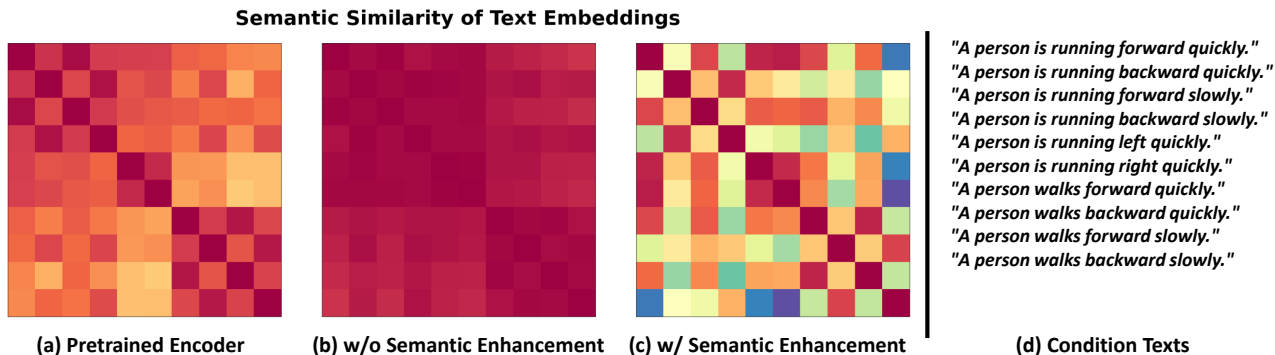


Figure 11. **Semantic Enhancement on Text Embedding.** We show the pairwise similarity of embeddings obtained by: (a) pretrained text encoder, (b) multimodal condition encoder trained w/o semantic enhancement, (c) multimodal condition encoder trained w/ semantic enhancement. (d) is the condition text descriptions.

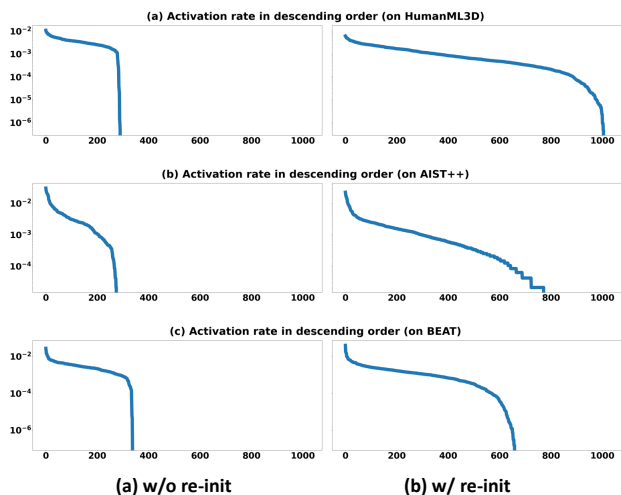


Figure 12. **Comparison of Activation Rate.** We investigate the effectiveness of weights re-initialization. We sort the activation rate in descending order. We use logarithm coordinates for y-axis.

two samples per genre. Each sample is a 4-second dance segment. For the speech-to-motion domain, we show samples of the generation of 4 speakers. We display the whole-body motions in the middle, and we enlarge the displays of left/right-hand movements at the side for convenience of visualization.

E. More Results of Diverse Generation

We show more results to demonstrate our method’s capability in synthesizing diverse motion with high condition consistency in Fig. 16, 17, 18. We synthesize 4 motion sequences from each condition signal to demonstrate the diversity of generation. We show diverse torso movements for text-to-motion and music-to-motion scenarios and present

both torch and hand movements for speech-to-motion scenarios. The results suggest that our method is able to synthesize not only diverse torch movements but also diverse and smooth hand movements.

F. Limitation and Future Work

1) Due to the limitation of dataset[10, 14], our method is currently not available for generating hand movements for text- and music-driven scenarios. Collecting datasets with richer annotation(e.g. [16]), as well as enabling the text- and music-conditioned hand motion synthesis is one of our prior future works. 2) Our method supports synthesizing a single person’s motion at this stage. Generating interactive actions conditioned on multimodal signals is of great value. This includes interacting with other persons or with the environment. Our future work also focuses on it. 3) Appropriate evaluation metrics are beneficial to further improvements. Our future work also lies in investigating better metrics.

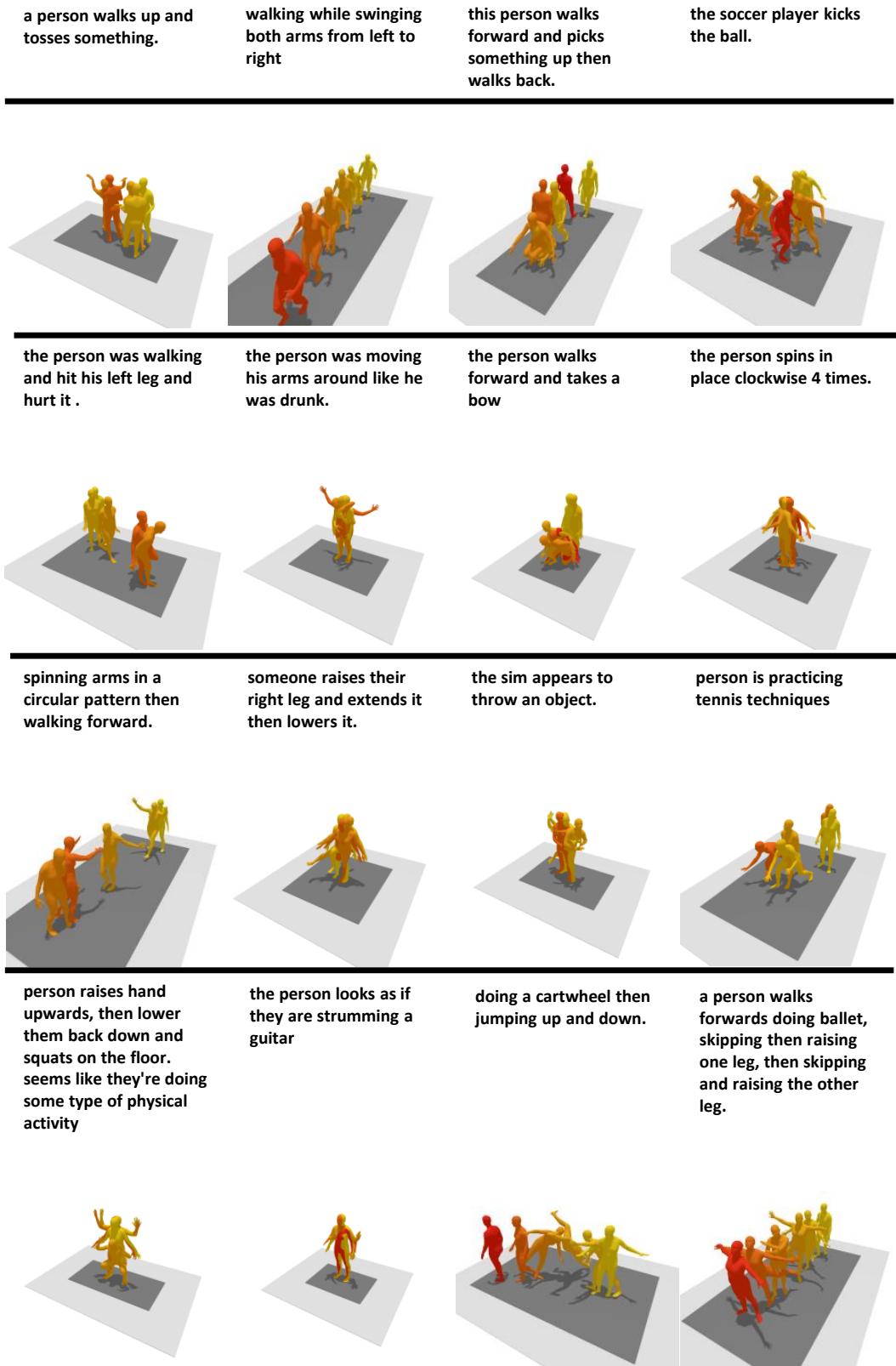


Figure 13. More Results on Text-to-Motion Generation.

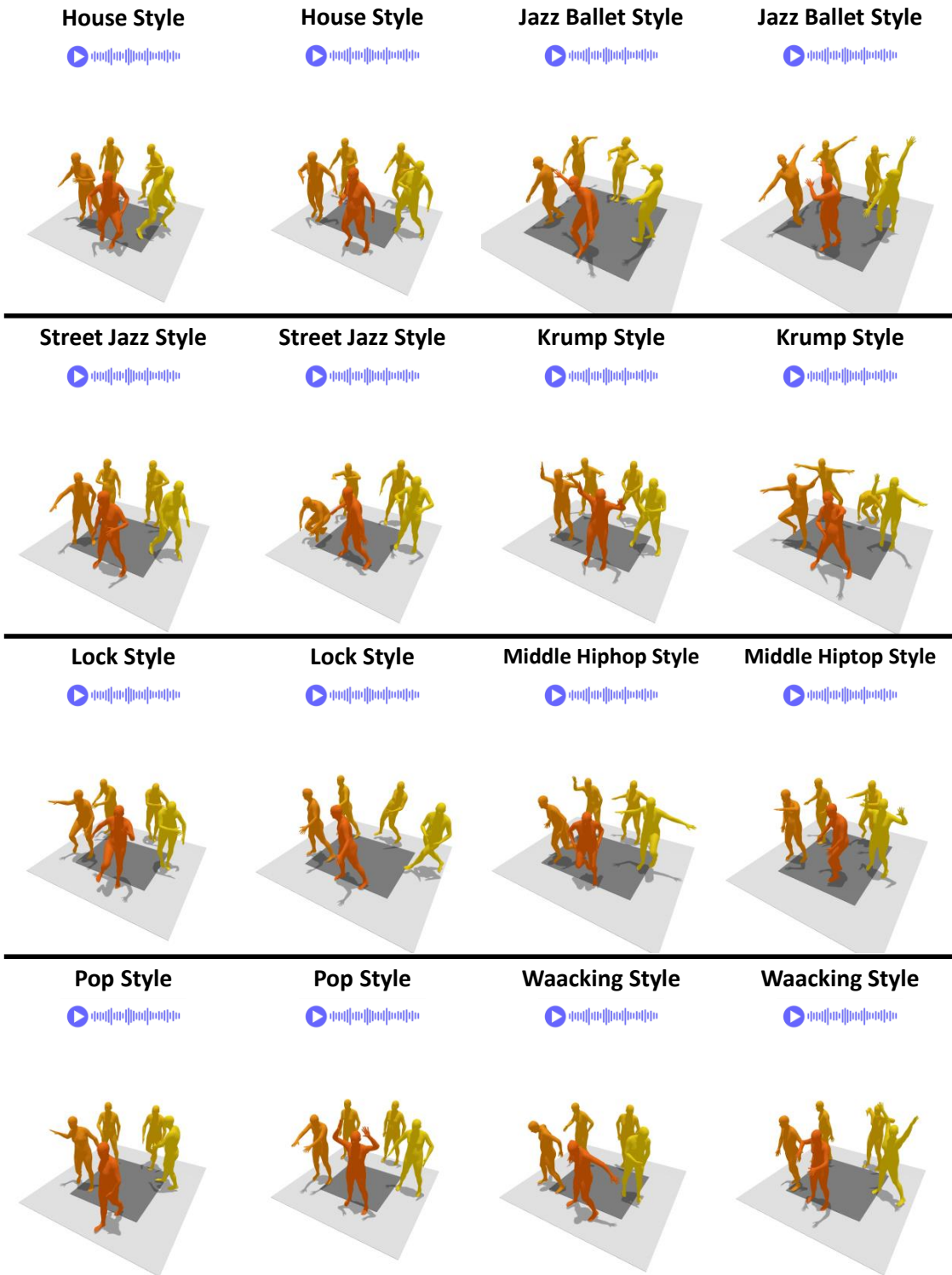


Figure 14. More Results on Music-to-Motion Generation.

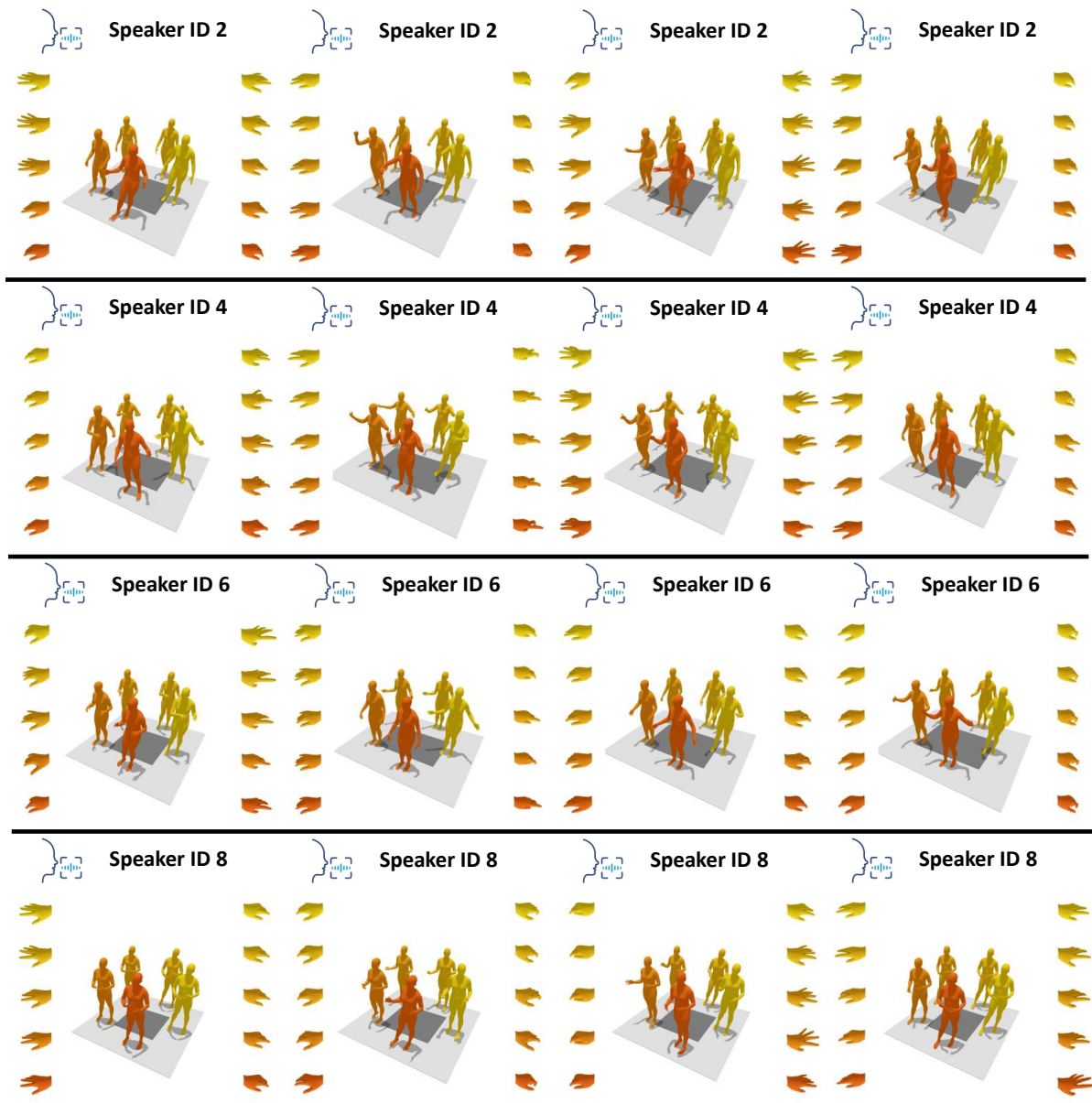
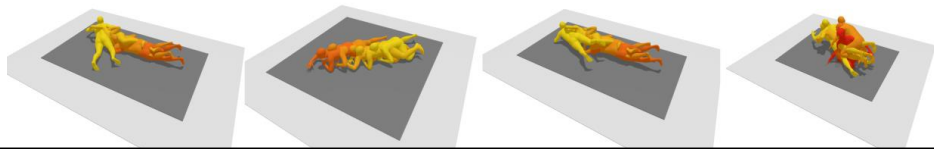
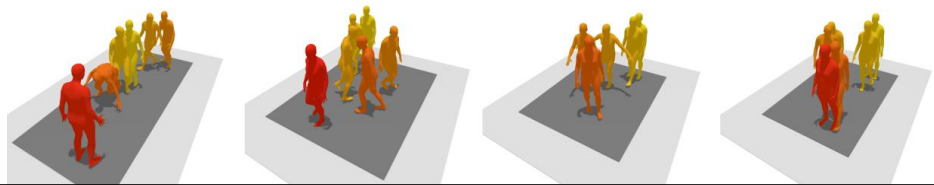


Figure 15. More Results on Speech-to-Motion Generation.

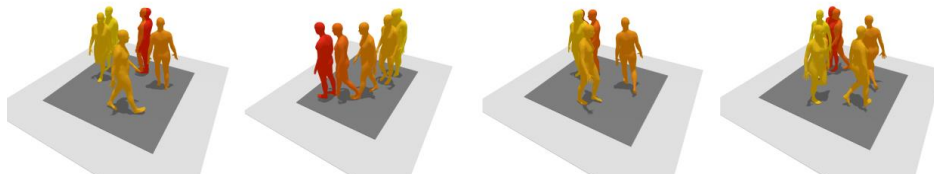
person is staying on the ground crawling back and forth.



walking in a random pattern.



this person walks in a counterclockwise direction.



the person is waving at something.



a character quickly walks forward in a diagonal motion then turns around and walks back to where they started.

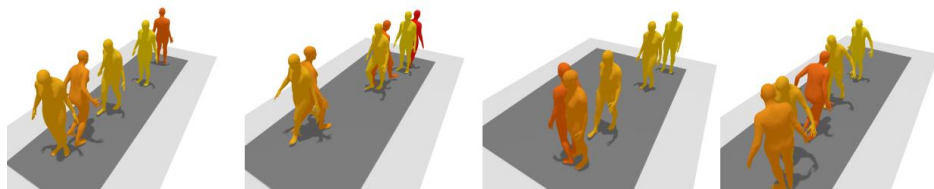


Figure 16. More Results on Diverse Text-to-Motion Generation.

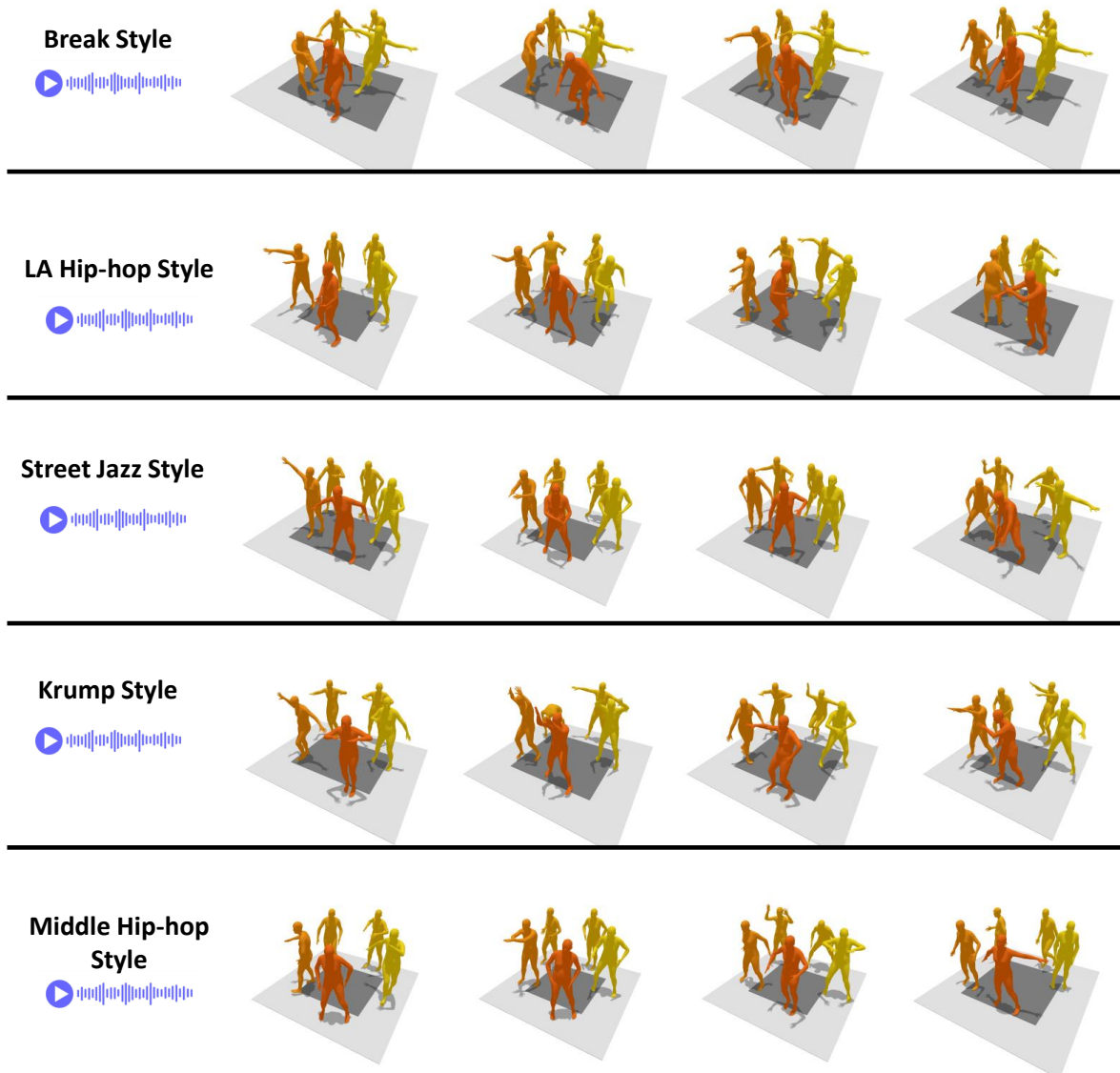


Figure 17. More Results on Diverse Music-to-Motion Generation.

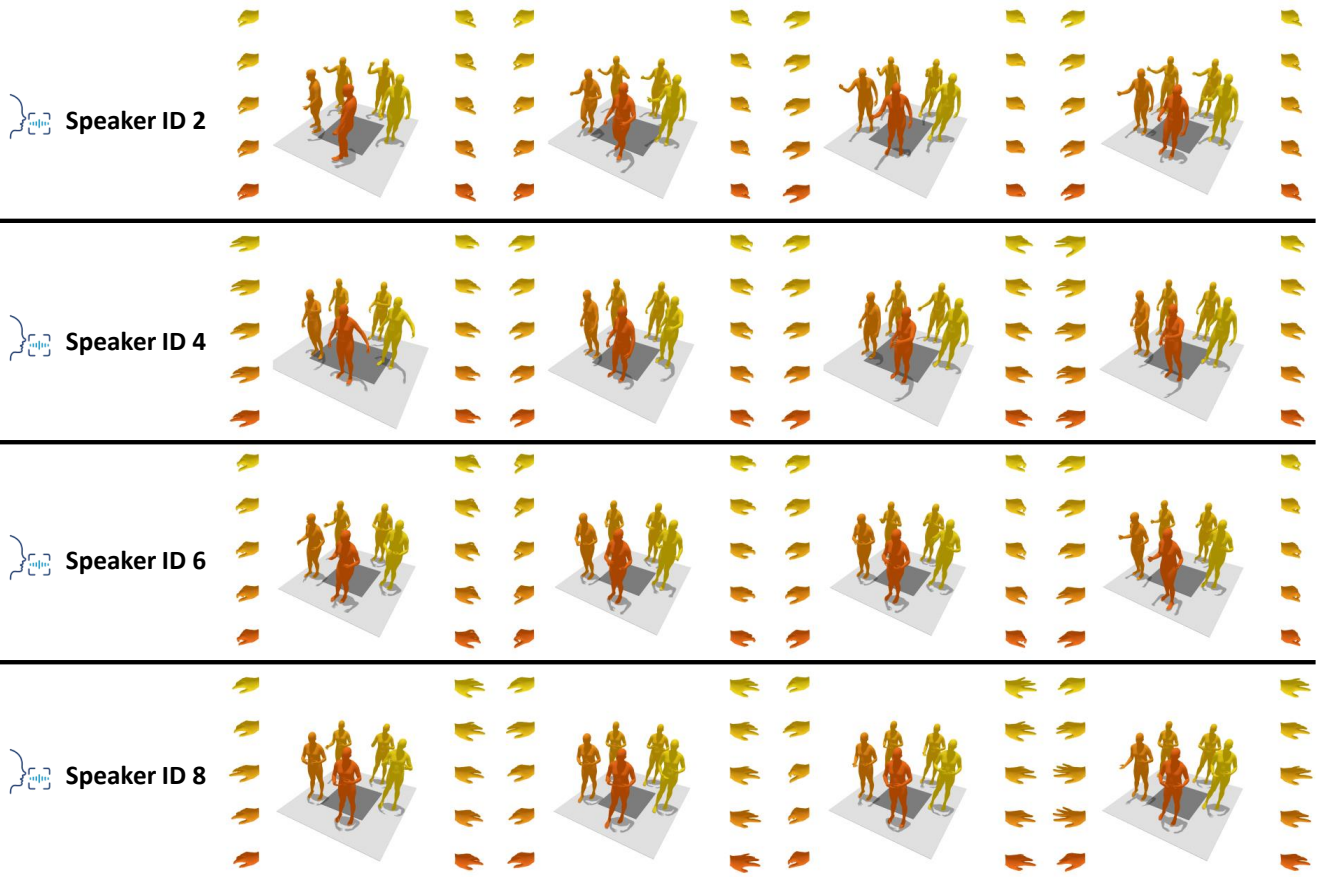


Figure 18. More Results on Diverse Speech-to-Motion Generation.